10.1071/WF21088
International Journal of Wildland Fire

Supplementary Material

Firebrand transport from a novel firebrand generator: numerical simulation of laboratory experiments

R. Wadhwani[A,B], *D. Sutherland*[B,C], *A. Ooi*[B,D] and *K. Moinuddin*[A,B,*]

[A]Centre for Environmental Safety and Risk Engineering, Victoria University, Melbourne, Vic. 3030, Australia

[B]Bushfire and Natural Hazards Cooperative Research Centre (CRC), Melbourne, Vic. 3002, Australia

[C]School of Science, University of New South Wales, Canberra, ACT 2600, Australia

[D]Department of Mechanical Engineering, University of Melbourne, Vic. 3052, Australia

*Correspondence to: Email: khalid.moinuddin@vu.edu.au

Experimental and numerical study of firebrand transport from a firebrand generator

R. Wadhwani[1,2,], D. Sutherland[2,3], A. Ooi[2,4], K. Moinuddin[1,2]*

[1]Centre for Environmental Safety and Risk Engineering, Victoria University, Melbourne, VIC 3030, Australia

[2]Bushfire and Natural Hazards CRC, Melbourne, VIC 3002, Australia

[3]School of Science, University of New South Wales, Canberra, ACT 2600, Australia

[4]Department of Mechanical Engineering, University of Melbourne, VIC 3052, Australia

Fig. S1-S4 shows a longitudinal normalised distribution of firebrand particles close to the centre i.e. in grid $y = -0.1\,m$ for both non-burning and burning firebrands at two Reynolds number. The figures are supplemental to the contour distribution presented in Fig. 5-8 in the manuscript.

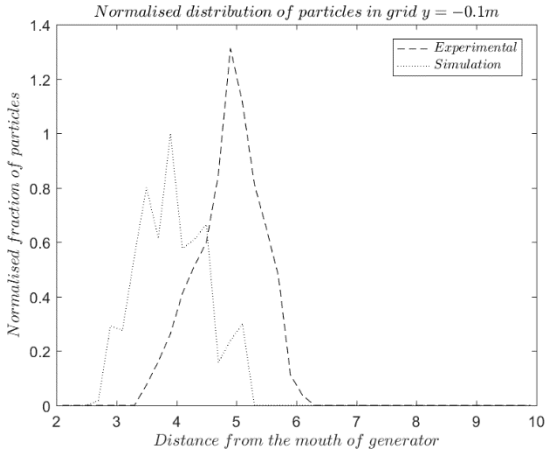

(a) Default FDS

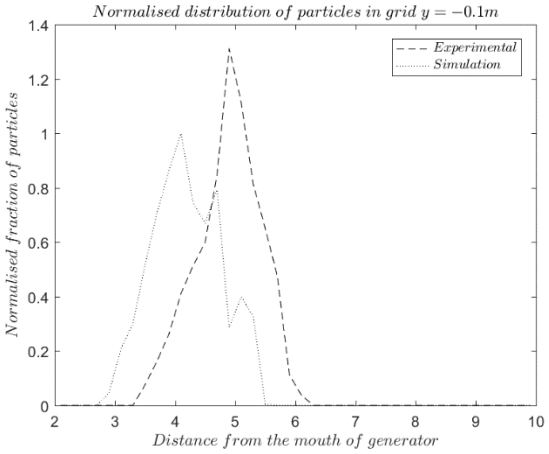

(b) Haider and Levenspiel

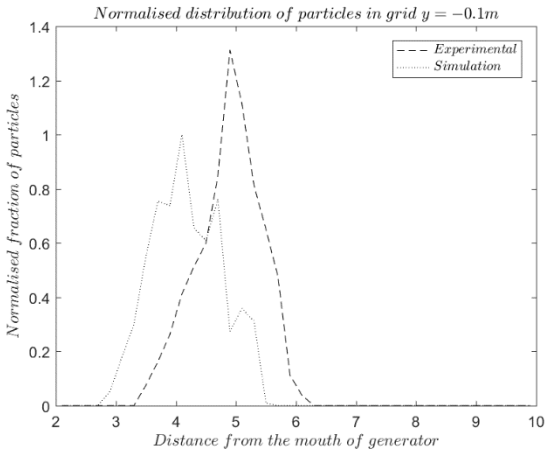

(c) Ganser

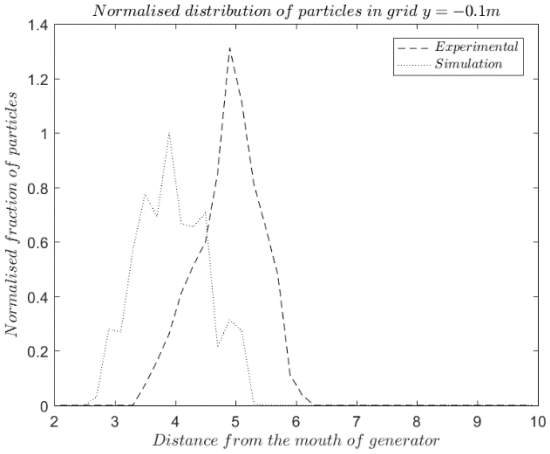

(d) Hölzer and Sommerfeld

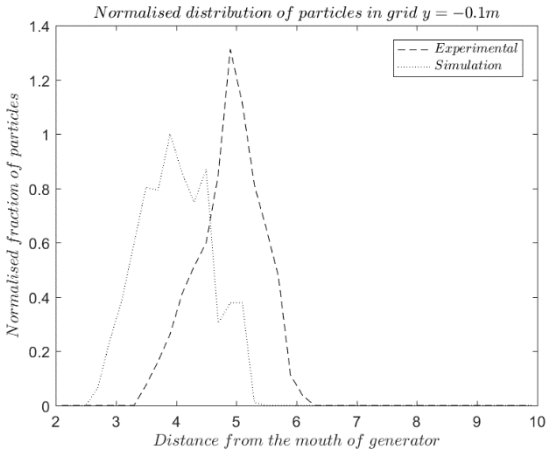

(e) Bagheri and Bonadonna

Fig. S1: Longitudinal distribution of non-burning at Re1 along y=-0.1m

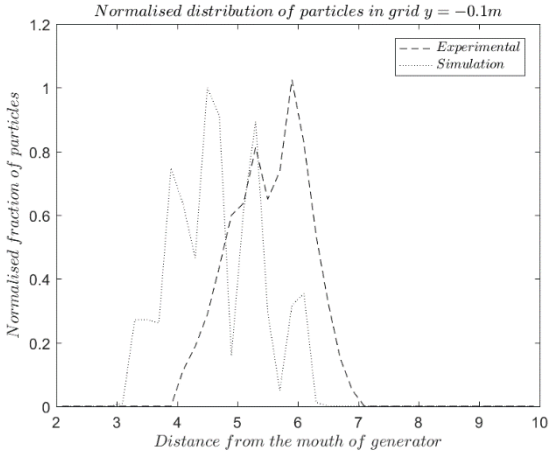

(a) Default FDS

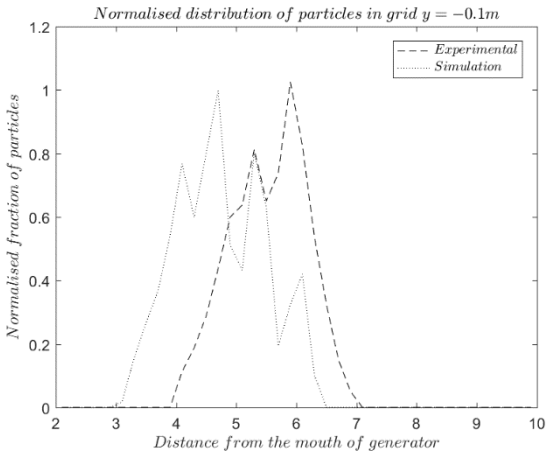

(b) Haider and Levenspiel

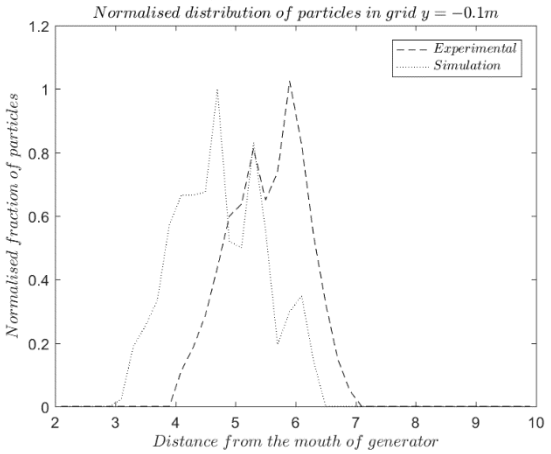

(c) Ganser

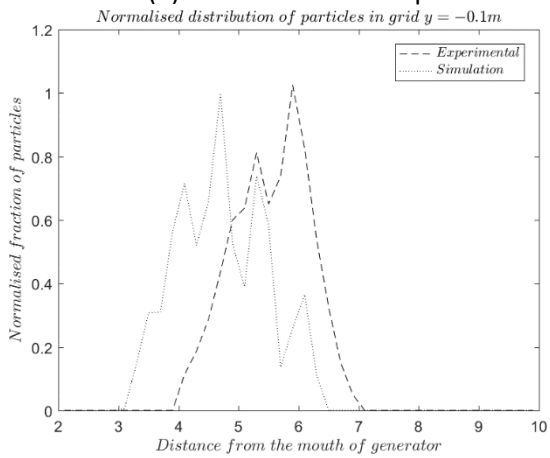

(d) Hölzer and Sommerfeld

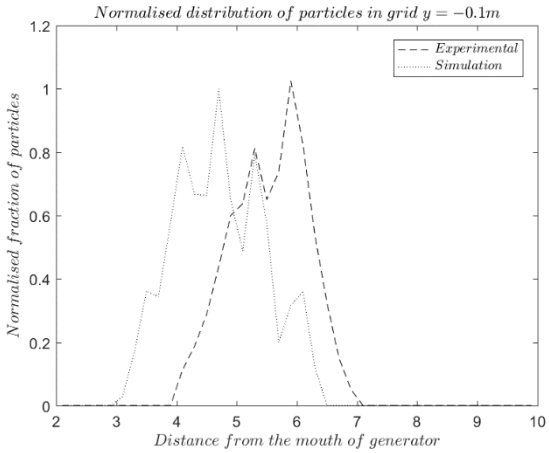

(e) Bagheri and Bonadonna

Fig. S2: Longitudinal distribution of non-burning at Re2 along y=-0.1m

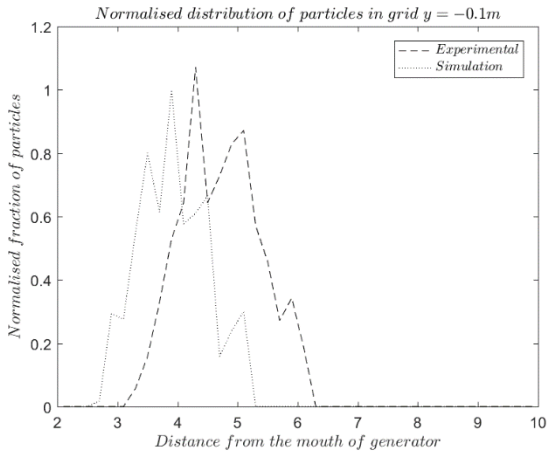

(a) Default FDS

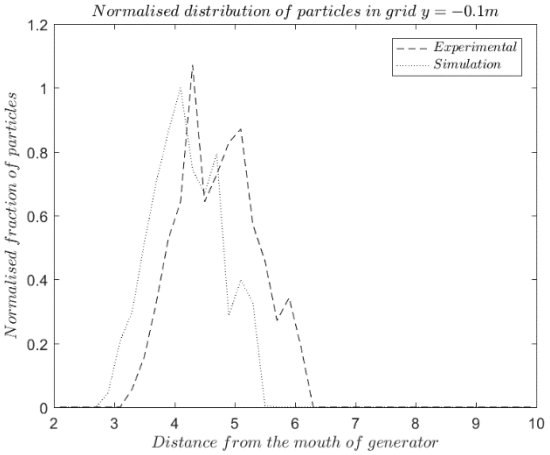

(b) Haider and Levenspiel

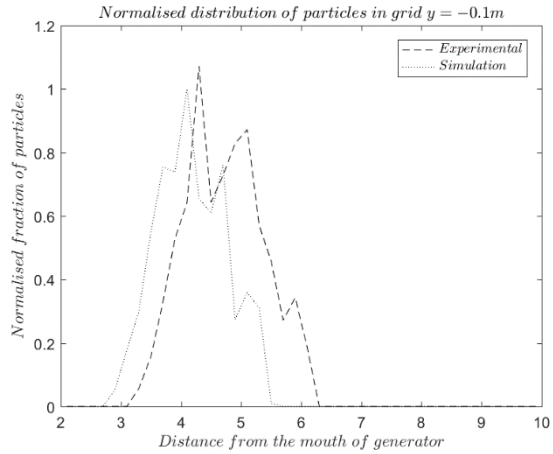

(c) Ganser

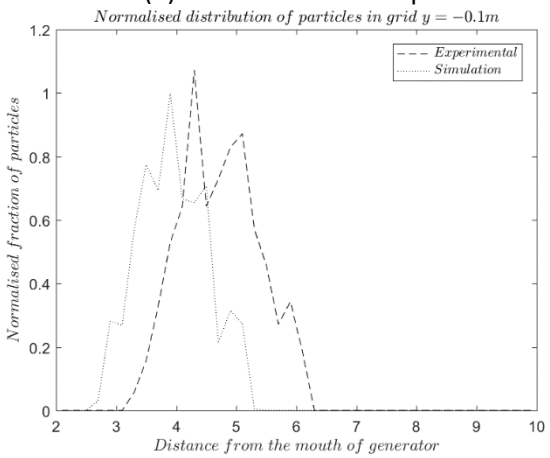

(d) Hölzer and Sommerfeld

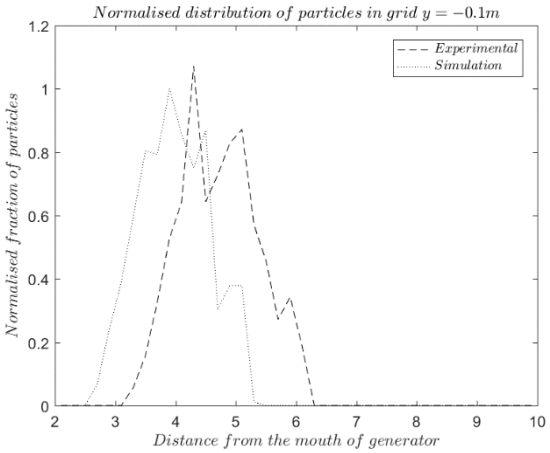

(e) Bagheri and Bonadonna

Fig. S3: Longitudinal distribution of burning at Re1 along y=-0.1m

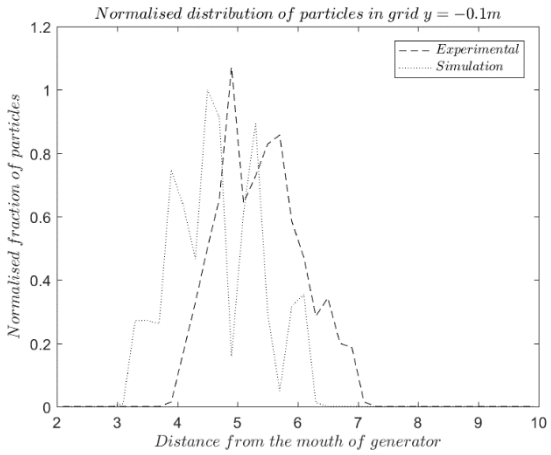

(a) Default FDS

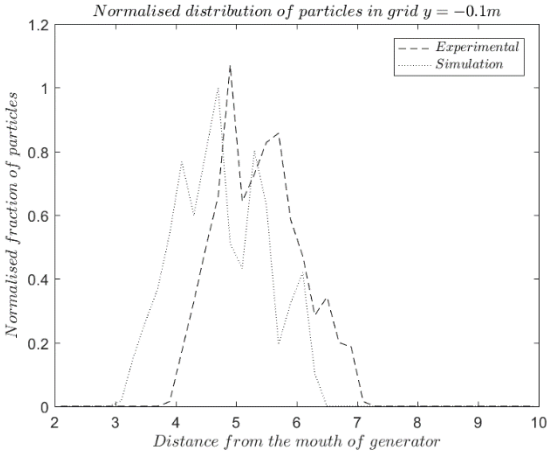

(b) Haider and Levenspiel

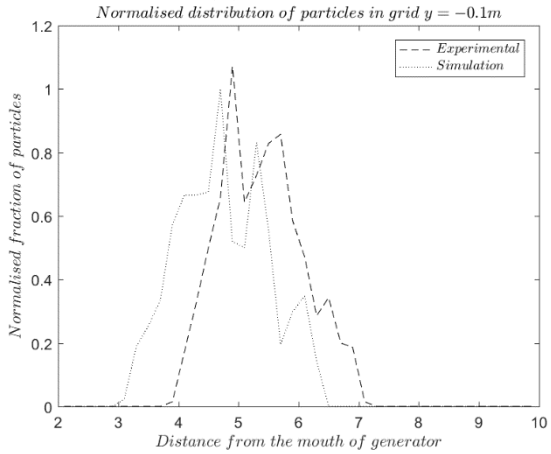

(c) Ganser

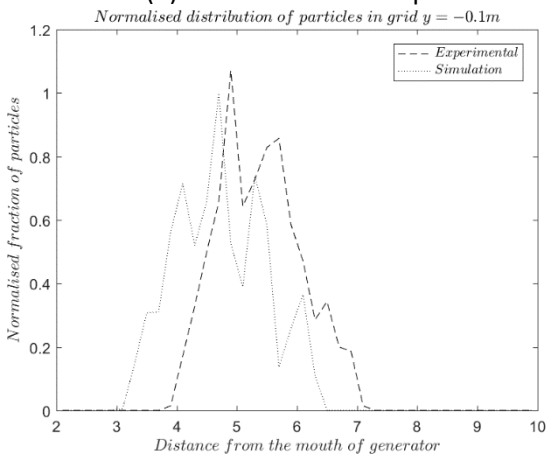

(d) Hölzer and Sommerfeld

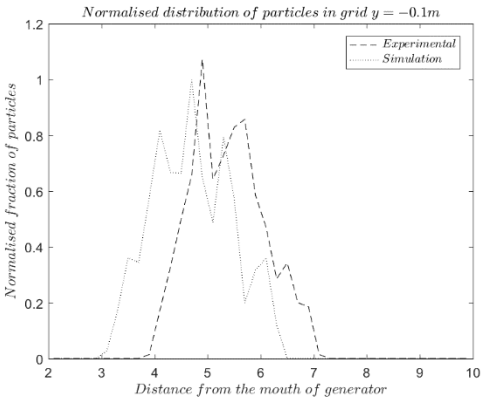

(e) Bagheri and Bonadonna

Fig. S4: Longitudinal distribution of burning at Re2 along y=-0.1m

Fig. S5-S8 presents a lateral distribution of particles along the peak position of experiment and simulation highlighting percentage of particle common in simulation and experiment at the peak location. The relative error is defined below which is on the basis of area under the curves (experimental, simulation and common shaded region)

$$Normalised\ relative\ error = \frac{\left|\frac{area_{exp}-area_{sim}}{area_{sim}}\right|}{\frac{area_{common}}{area_{exp}}} \times 100\ .$$

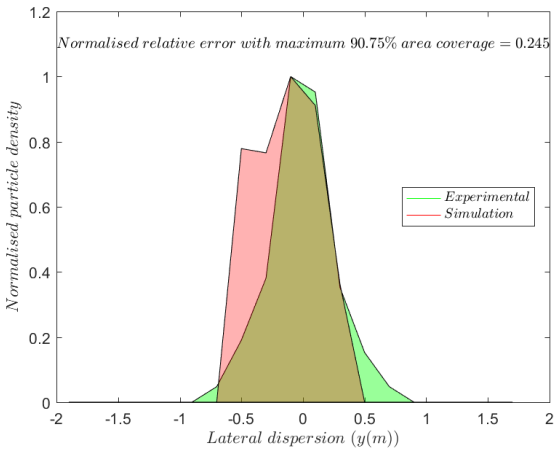

(a) Default FDS

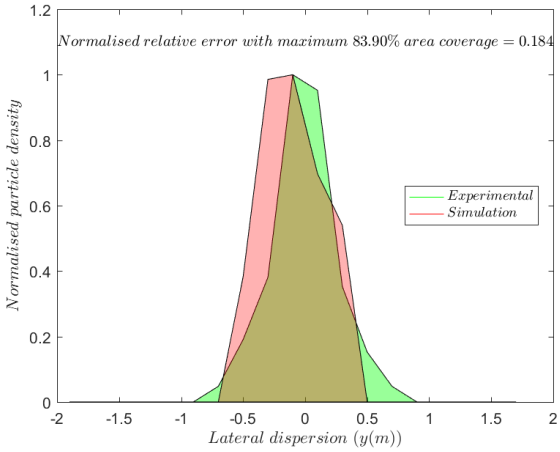

(b) Haider and Levenspiel

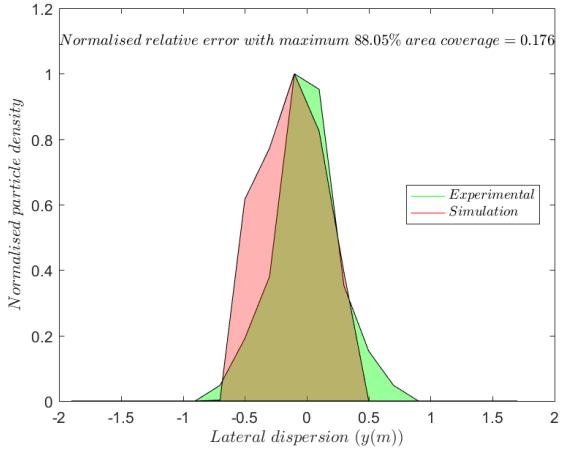

(c) Ganser

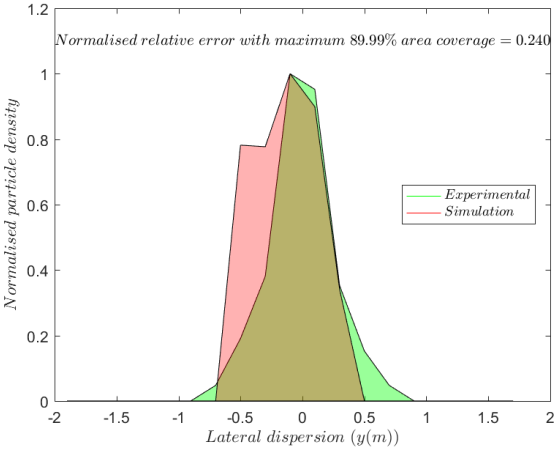

(d) Hölzer and Sommerfeld

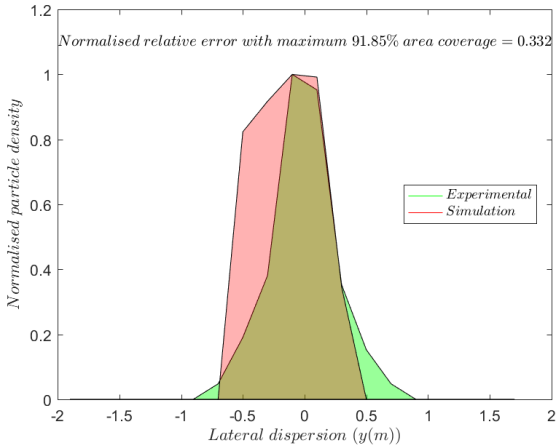

(e) Bagheri and Bonadonna

Fig. S5: Lateral distribution of non-burning at Re1 at the peak location

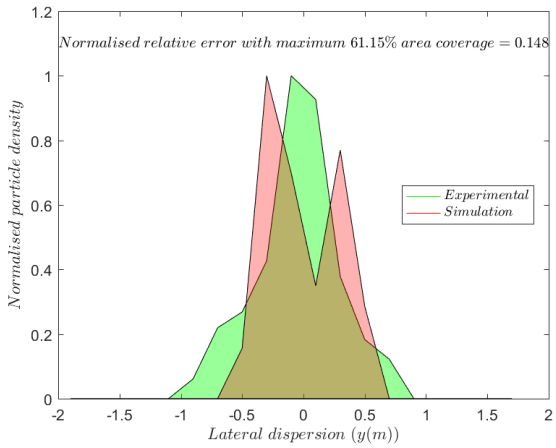

(a) Default FDS

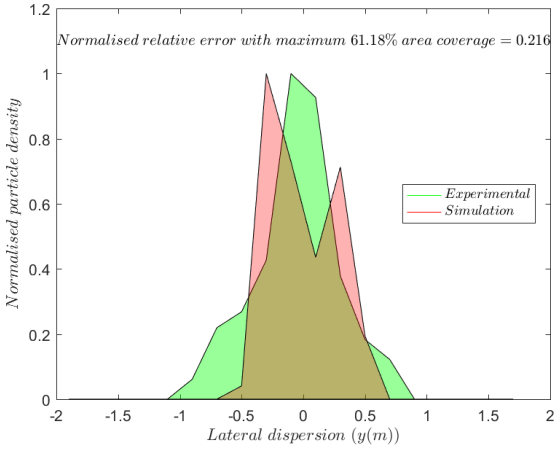

(b) Haider and Levenspiel

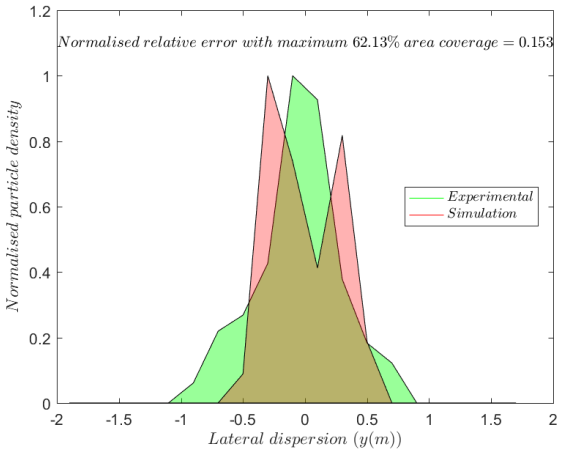

(c) Ganser

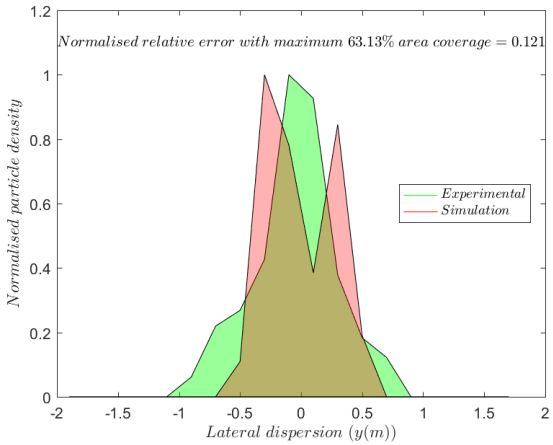

(d) Hölzer and Sommerfeld

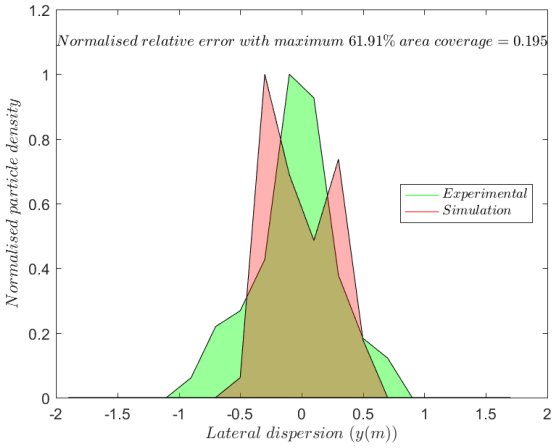

(e) Bagheri and Bonadonna

Fig. S6: Lateral distribution of non-burning at Re2 at the peak location

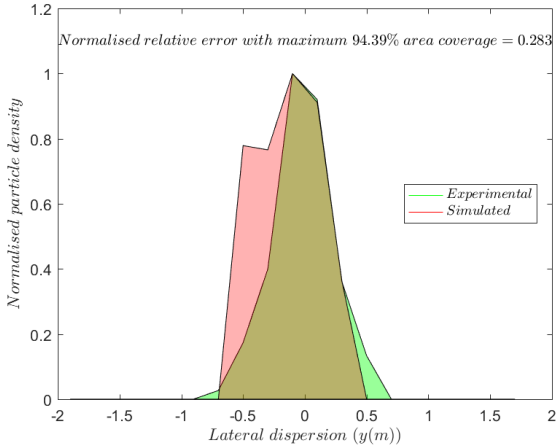

(a) Default FDS

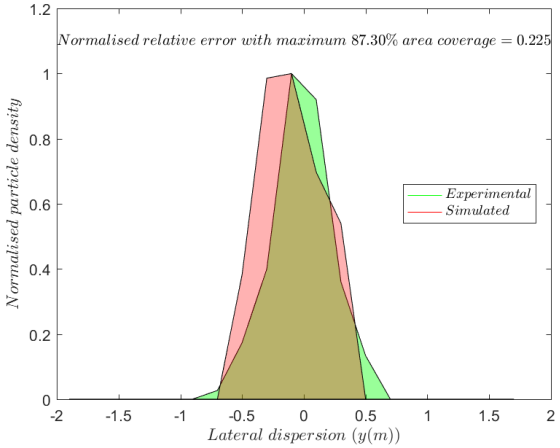

(b) Haider and Levenspiel

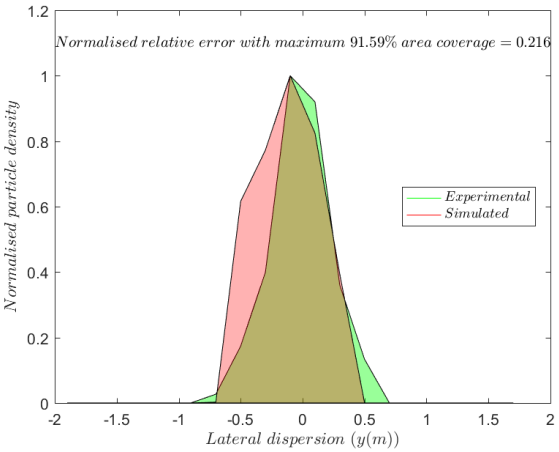

(c) Ganser

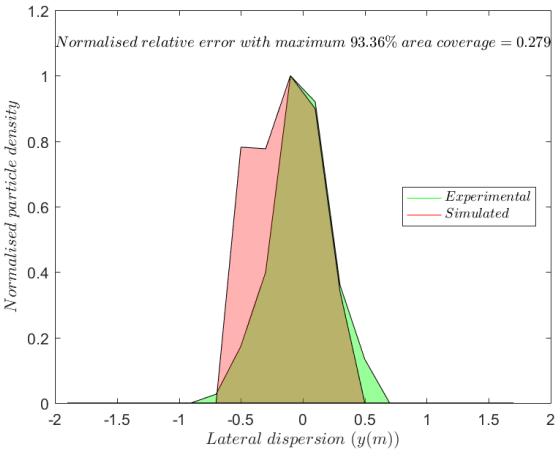

(d) Hölzer and Sommerfeld

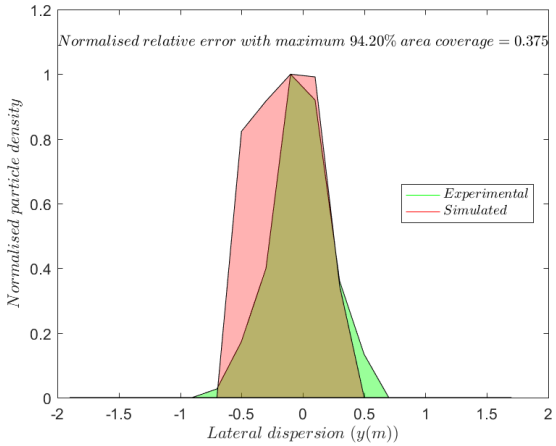

Fig. S7: Lateral distribution of burning at Re1 at the peak location

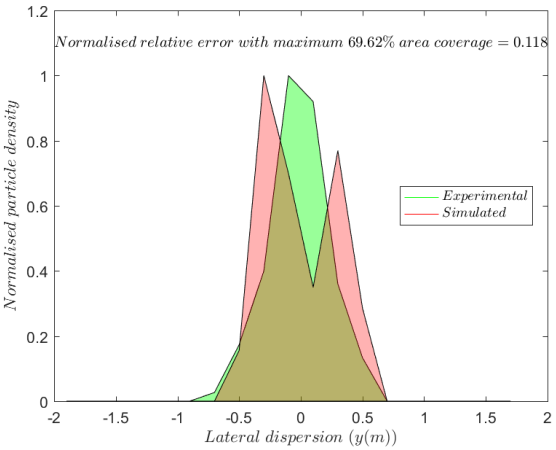

(a) Default FDS

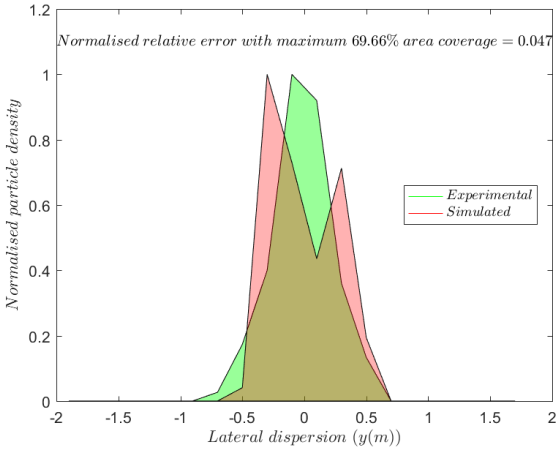

(b) Haider and Levenspiel

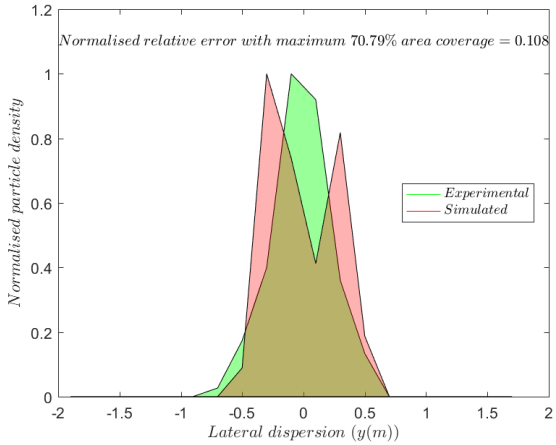

(c) Ganser

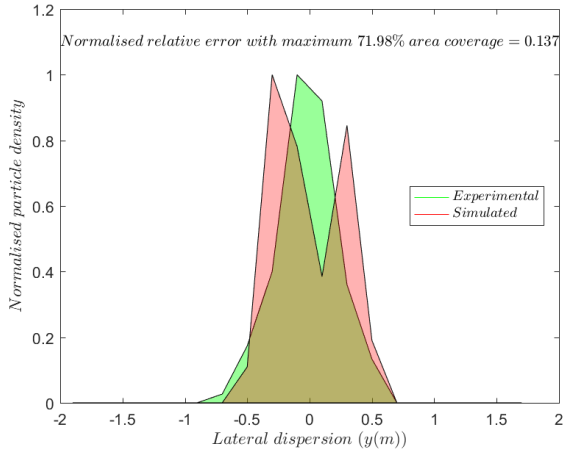

(d) Hölzer and Sommerfeld

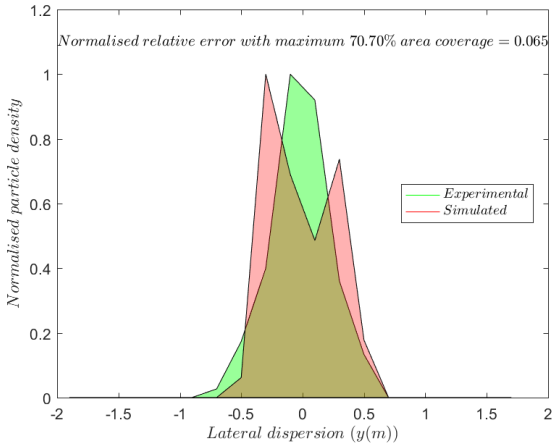

(e) Bagheri and Bonadonna

Fig. S8: Lateral distribution of burning at Re2 at the peak location

Figs. S9-S12 show the cumulative distribution functions (CDF) of particles as a function of distance from the peak location for all cases. To obtain the CDF, the location (x_0, y_0) of the maximum of the particle landing distribution was obtained. The coordinates of each particle (x_i, y_i) landing location was obtained. The (x_i, y_i) were then converted to cylindrical polar coordinates centred at (x_0, y_0) and the resulting (r_i, θ_i) distribution was averaged in the azimuthal direction. This gives a one-dimensional distribution of particles as a function of distance from the peak location. This distance data, for both the experimental and simulated distributions, was sorted into 20 histogram bins, the cumulative sum of the data was computed, and appropriately normalised to give the CDF. 20 histogram bins adequately capture the landing distribution. The Kolmogorov-Smirnov (KS) test was be applied to these CDF. The null hypothesis was that the observations are from the same underlying distribution. The test statistic, $S = max(|CDF_{exp} - CDF_{sim}|)$. To reject the null hypothesis at significance level alpha the test statistic must be:

$$S > c(\alpha)\left(\frac{m+n}{mn}\right)^{1/2}$$

$c(\alpha)$ is some constant for the significance level, m and n are the sample sizes ($n = m = 20$ bins in this case). To reject the null hypothesis at 10% significance ($c = 1.224$ [S1]) requires $S > 0.38$. From the figures, the maximum value of the test statistic across all distributions was approximately $S = 0.1$, which is insufficient to reject the null hypothesis. However, this test is on azimuthally averaged data and so information about the radial distribution of the particles is lost. The KS test only affirms that the experimental and simulated distributions are indistinguishable and does not provide insight into the quality of the individual methods.

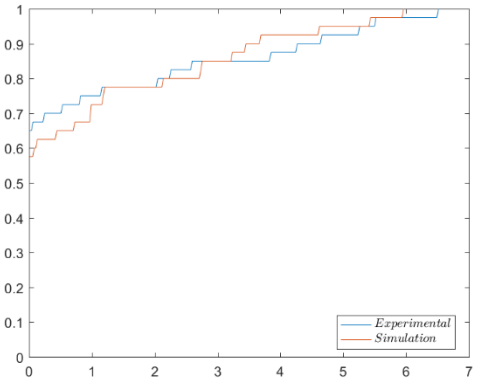

(f) Default FDS

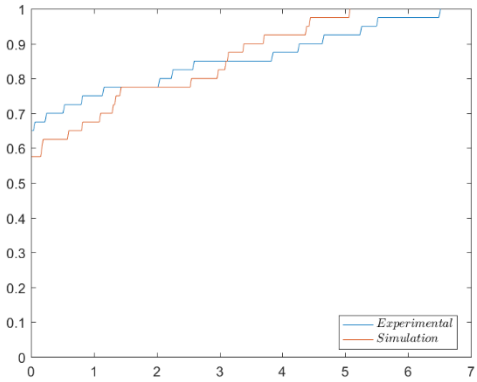

(g) Haider and Levenspiel

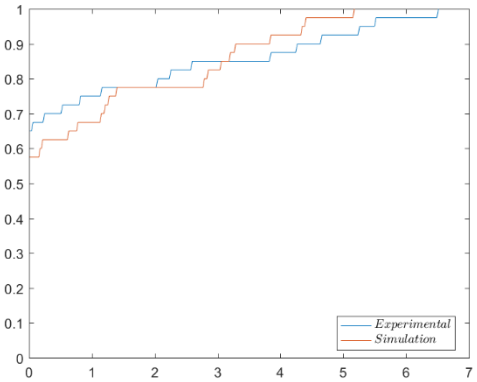

(h) Ganser

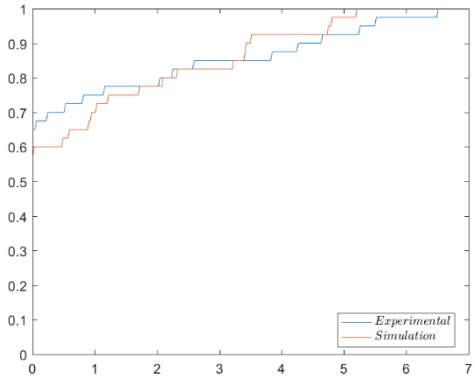

(i) Hölzer and Sommerfeld

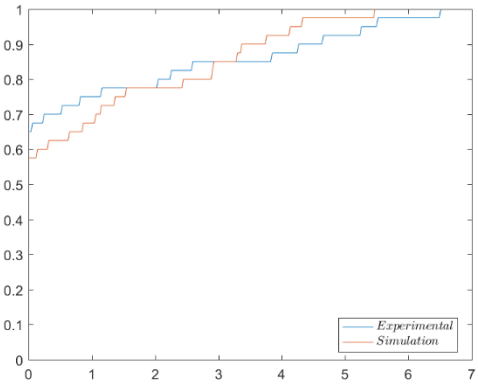

(j) Bagheri and Bonadonna

Fig. S9: CDF of non-burning at Re1

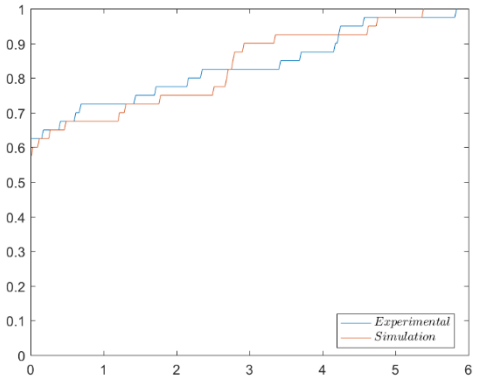

(a) Default FDS

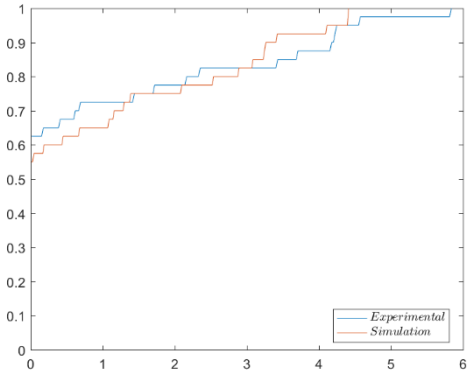

(b) Haider and Levenspiel

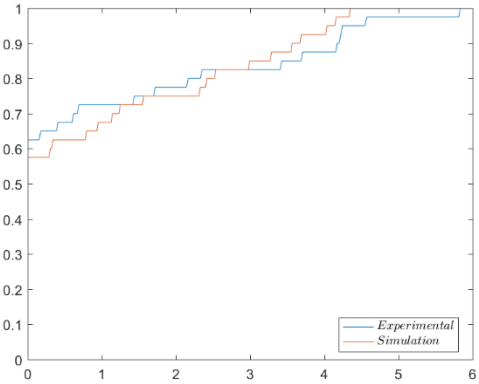

(c) Ganser

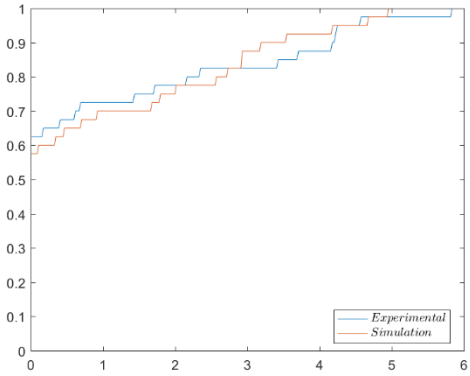

(d) Hölzer and Sommerfeld

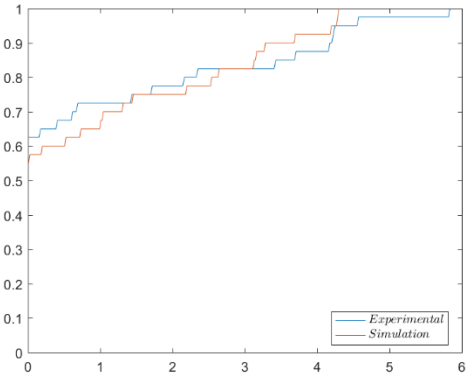

(e) Bagheri and Bonadonna

Fig. S10: CDF of non-burning at Re2

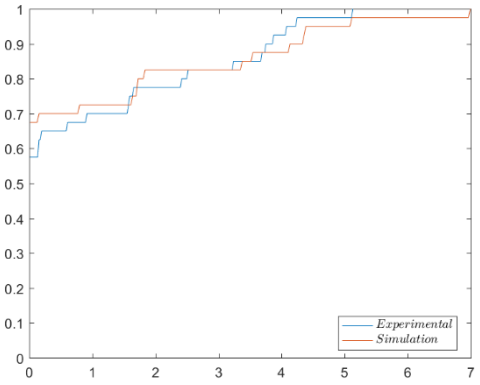

(a) Default FDS

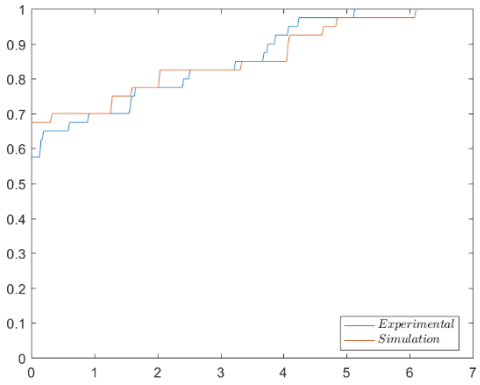

(b) Haider and Levenspiel

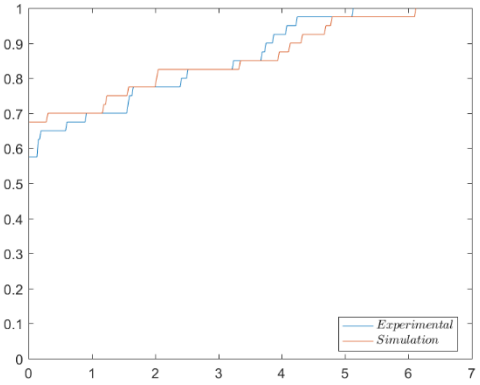

(c) Ganser

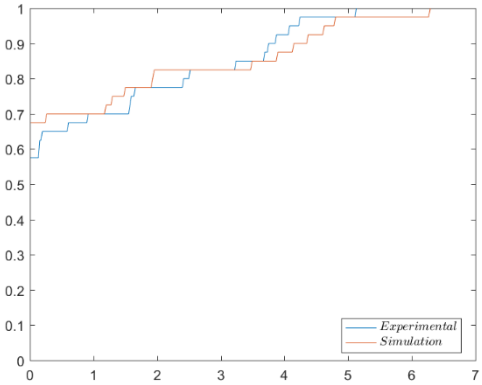

(d) Hölzer and Sommerfeld

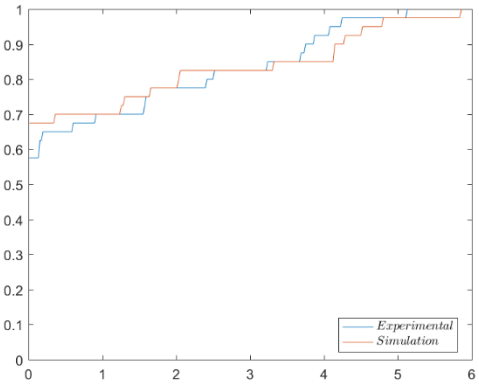

Fig. S11: CDF of burning at Re1

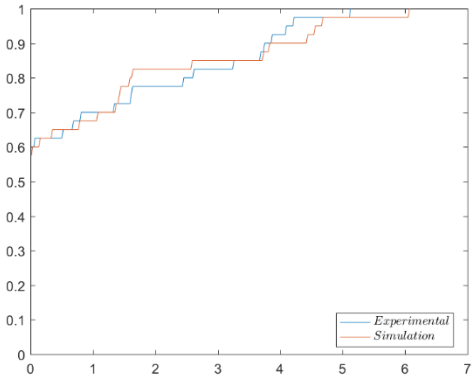

(a) Default FDS

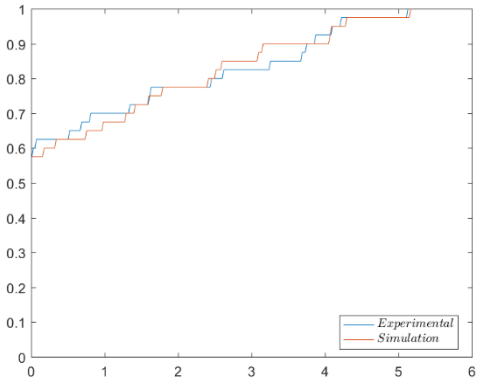

(b) Haider and Levenspiel

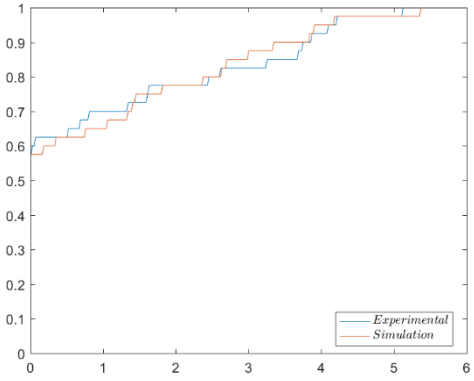

(c) Ganser

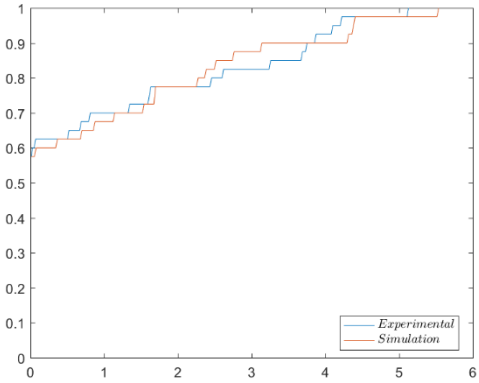

(d) Hölzer and Sommerfeld

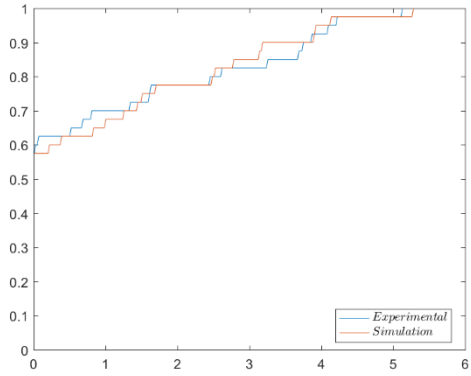

(e) Bagheri and Bonadonna

Fig. S12: CDF of burning at Re2

Reference:

S1 Miller, LH (1956). Table of percentage points of Kolmogorov statistics. *Journal of the American Statistical Association*, **51(273)**, 111-121.